

## Structure and Stability of Sodium Intercalated Phases in Olivine $\text{FePO}_4$

P. Moreau,\* D. Guyomard, J. Gaubicher, and F. Boucher

*Institut des Matériaux Jean Rouxel (IMN), Université de Nantes, CNRS, 2 rue de la Houssinière, BP 32229, 44322 Nantes cedex 3, France*

*Received May 15, 2010*

*Revised Manuscript Received June 23, 2010*

Numerous publications exist concerning  $\text{LiFePO}_4$ , especially with regard to its remarkable electrochemical storage properties.<sup>1</sup> Aside from research in the field of phosphate-based water treatments for high pressure steam generators,<sup>2</sup>  $\text{NaFePO}_4$ , the chemical equivalent with sodium, has not been as extensively explored.<sup>3</sup> The typical  $\text{NaFePO}_4$  maricite phase seems to be the thermodynamically favored phase because it is obtained at high temperature or in hydrothermal conditions.<sup>2,4</sup> The maricite phase, however, presents one-dimensional, edge-sharing  $\text{FeO}_6$  octahedrons and no cationic channels (Figure 1a), contrary to the olivine  $\text{LiFePO}_4$  (Figure 1b). An olivine-based  $\text{NaFePO}_4$  phase would therefore be particularly interesting in order to study its electrochemical properties, especially in the context of the renewed interest for sodium batteries.<sup>5</sup> Possible physical new properties of a sodium-deficient phase could also be of interest, much like  $\text{Na}_x\text{CoO}_2$ , following the discovery of supraconductivity or thermoelectric properties in its derivatives.<sup>6</sup> Because the direct synthesis of the olivine phase seems unfavorable, the cation exchange from  $\text{LiFePO}_4$  is the logical way forward. This process of synthesis was shown to be effective for the electrochemical insertion of sodium in  $\text{FePO}_4$  (olivine  $Pnma$ ).<sup>3a,b</sup> Surprisingly, the resulting structure is still unpublished and no intermediate phase was reported. If one is to understand the fundamental differences between the insertion of lithium versus sodium in similar host materials, as well as study the stability and properties of such phases, precise structural determinations are essential. This communication

presents the resolution of the  $\text{NaFePO}_4$  olivine structure, along with that of an intermediate phase,  $\text{Na}_{0.7}\text{FePO}_4$ , obtained during the charge of a sodium battery. Both ab initio calculations, as well as thermal analyses, illustrate the relative stabilities of the electrochemically prepared phases.

Sodium intercalated samples were synthesized electrochemically using a positive electrode made with a mixture of 70%  $\text{FePO}_4$  (olivine) and 30% carbon black (Ketjen).  $\text{FePO}_4$  was obtained from  $\text{LiFePO}_4$ ,<sup>7</sup> by chemical oxidation in acetonitrile using  $\text{NO}_2\text{BF}_4$ .<sup>8</sup> The mixture was ball-milled (30 min, 500 rpm) and pasted onto an Al current collector. Swagelok-type batteries were mounted with sodium as the negative and reference electrode and EC: PC (50/50) 1 M  $\text{NaClO}_4$  as the electrolyte. Batteries were cycled in potentiodynamic mode (PITT) with time steps being limited by a current limit. The latter was set equivalent to 1 Na/50 h for cycling experiments and 1 Na/200 h when equilibration of samples was performed prior to XRD analysis. In this case, powders were recovered at different stages of the cycling curve (Figure 2) and analyzed by ex situ X-ray diffraction on a D5000 diffractometer. Whether starting from noncarbon or carbon-coated  $\text{LiFePO}_4$ , or using galvanostatic or potentiodynamic mode, electrochemical results were identical.

The complete sodiation of the  $\text{FePO}_4$  olivine is obtained and is reversible. Unlike the Li/ $\text{FePO}_4$  system, however, it occurs in two steps, with the formation of the intermediate  $\text{Na}_{0.7}\text{FePO}_4$  composition (Figure 2). X-ray diffraction patterns at the end of the charge (point C in Figure 2) lead to the same olivine structure as the pristine  $\text{FePO}_4$  structure. The atomic structure of the fully intercalated compound (point A in Figure 2) was obtained by Rietveld refinement of the X-ray diffraction diagram (Figure 3).<sup>9</sup> The sodium site occupancy was refined as 1.003(12), confirming the full intercalation.  $\text{NaFePO}_4$  cell parameters are slightly larger than for the lithium equivalent:  $a = 10.4063(6)$  Å,  $b = 6.2187(3)$  Å,  $c = 4.9469(3)$  Å and  $V = 320.14(3)$  Å<sup>3</sup> (compared to  $a = 10.332(4)$  Å,  $b = 6.010(5)$  Å,  $c = 4.692(2)$  Å, and  $V = 291.35(10)$  Å<sup>3</sup> for  $\text{LiFePO}_4$ ).<sup>10</sup> The  $\sim 0.2$  Å increase for the  $b$  and  $c$  axes is consistent with that of ionic radii from lithium (90 pm) to sodium (116 pm). The  $a$  parameter, on the contrary, increases only by 0.07 Å. In this direction,  $\text{FeO}_6$  octahedrons are linked by  $\text{PO}_4$  tetrahedrons, which are known for being particularly rigid entities. Bond valence sums (BVS) calculated using the charge distribution procedure

\*Corresponding author.

- (1) (a) Padhi, A. K.; Nanjundaswamy, K. S.; Goodenough, J. B. *J. Electrochem. Soc.* **1997**, *144*, 1188–1194. (b) Scrosati, B.; Garche, J. *J. Power Sources* **2010**, *195*, 2419–2430.
- (2) Tremaine, P. R.; Xiao, C. *J. Chem. Thermodyn.* **1999**, *31*, 1307–1320.
- (3) (a) Le Poul, N.; Baudrin, E.; Morcrette, M.; Gwizdala, S.; Masquelier, C.; Tarascon, J. M. *Solid State Ionics* **2003**, *159*, 149–158. (b) Burba, C. M.; Frech, R. *Spectrochim. Acta, Part A* **2006**, *65*, 44–50. (c) Shiratsuchi, T.; Okada, S.; Yamaki, J.; Nishida, T. *J. Power Sources* **2006**, *159*, 268–271.
- (4) (a) Paques-Ledent, M. T. *Rev. Chim. Minér.* **1973**, *10*, 785. (b) Bridson, J. N.; Quinlan, S. E.; Tremaine, P. R. *Chem. Mater.* **1998**, *10*, 763–768.
- (5) Nishijima, M.; Gocheva, I. D.; Okada, S.; Doi, T.; Yamaki, J.-i.; Nishida, T. *J. Power Sources* **2009**, *190*, 558–562.
- (6) Kaurav, N.; Wu, K. K.; Kuo, Y. K.; Shu, G. J.; Chou, F. C. *Phys. Rev. B* **2009**, *79*, 075105.

- (7) Kobayashi, G.; Nishimura, S.-i.; Park, M.-S.; Kanno, R.; Yashima, M.; Ida, T.; Yamada, A. *Adv. Funct. Mater.* **2009**, *19*, 395–403.
- (8) Wizansky, A. R.; Rauch, P. E.; Disalvo, F. J. *J. Solid State Chem.* **1989**, *81*, 203–207.
- (9) Petricek, V.; Dusek, M.; Palatinus, L. *Jana 2006*; Institute of Physics: Praha, Czech Republic, 2006.
- (10) Streltsov, V. A.; Belokoneva, E. L.; Tsirelson, V. G.; Hansen, N. K. *Acta Cryst. B* **1993**, *49*, 147–153.

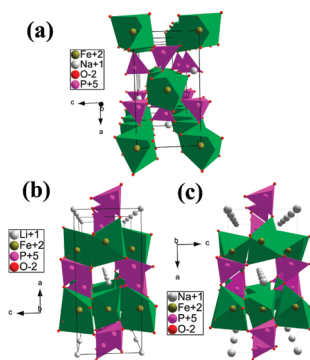


**Figure 1.** Structure of (a) maricite  $\text{NaFePO}_4$ , (b) olivine  $\text{LiFePO}_4$ , and (c) olivine  $\text{NaFePO}_4$ .

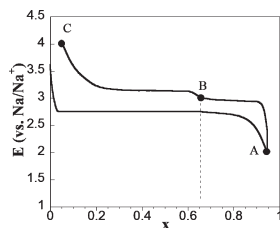


**Figure 2.** Typical electrochemical curve for the synthesis of  $\text{NaFePO}_4$  and  $\text{Na}_{0.7}\text{FePO}_4$  in PITT mode.

are in perfect agreement with expected values ( $\text{BVS}_{\text{Na}} = 0.995$ ,  $\text{BVS}_{\text{Fe}} = 2.005$ ,  $\text{BVS}_{\text{P}} = 5.001$ ).<sup>11</sup> One can thus be very confident concerning the quality of the structural description. Although the average value of Fe–O distances within the octahedrons are very similar in both olivine structures (2.1567(15) Å for  $\text{LiFePO}_4$  compared to 2.185(9) Å for  $\text{NaFePO}_4$ ), the octahedron distortion in the sodium compound is much higher. The distortion parameters ( $\Delta$ ,  $\lambda$ ,  $\sigma$ ),<sup>12</sup> already significant for the  $\text{FeO}_6$  octahedron in  $\text{LiFePO}_4$  ( $1.4 \times 10^{-3}$ , 1.045, 156), increase noticeably ( $2.1 \times 10^{-3}$ , 1.065, 217) in  $\text{NaFePO}_4$ . On the contrary,  $\text{PO}_4$  tetrahedrons, while presenting a little bond-angle distortion, are not affected by the replacement of lithium for sodium. Very similar ( $\Delta$ ,  $\lambda$ ,  $\sigma$ ) values are found in  $\text{LiFePO}_4$  ( $8.1 \times 10^{-5}$ , 1.004, 19) and  $\text{NaFePO}_4$  ( $4.1 \times 10^{-6}$ , 1.004, 18). The relative stability of this olivine-based  $\text{NaFePO}_4$  structure with respect to the well-known maricite structure was studied using thermal differential analysis. The positive electrode mixture was placed in a platinum crucible and heated up to 650 °C. An exothermic peak at around 488 °C was obtained on heating but was found to be not reversible (Figure 4, inset). Temperature-dependent in situ X-ray diffraction diagrams under nitrogen gas confirm the transition around 480 °C on heating and prove the transformation of the olivine phase into the

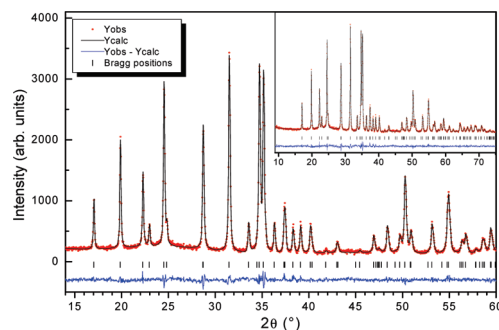


**Figure 3.** Rietveld refinement of  $\text{NaFePO}_4$  olivine structure obtained after full Na intercalation in  $\text{FePO}_4$ .

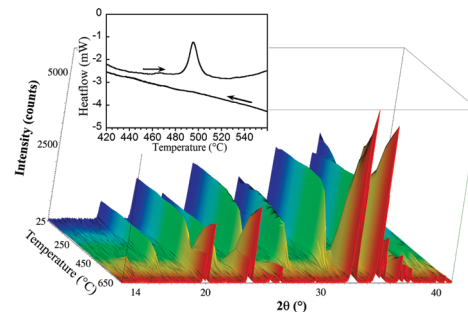


**Figure 4.** In situ X-ray diffraction patterns of the olivine  $\text{NaFePO}_4$  phase, for an increasing temperature from 25 to 650 °C. Inset: Thermal differential analysis of the  $\text{NaFePO}_4$  olivine phase.

maricite phase. Up to the transition, both  $b$  and  $c$  parameters expand regularly with to the first order  $\Delta b/T = +21.4(4) \times 10^{-5} \text{ Å K}^{-1}$  and  $\Delta c/T = +9.9(1) \times 10^{-5} \text{ Å K}^{-1}$ , whereas the  $a$  parameter slowly decreases with  $\Delta a/T = -2.4(2) \times 10^{-5} \text{ Å K}^{-1}$  (see the Supporting Information). This result should be linked once again to the high rigidity of  $\text{PO}_4$  tetrahedrons. At the olivine to maricite transition, a significant volume shrinkage is observed.

Stability of both olivine and maricite  $\text{NaFePO}_4$  phases were also studied by calculations of their respective total energies. The computer program VASP in the GGA+U approximation was used considering antiferromagnetic orders and  $U_{\text{eff}}$  parameters identical to those used for the treatment of the  $\text{LiFePO}_4$  olivine structure (details in the Supporting Information). The maricite phase is found to be 0.016 eV/formula unit more stable than the olivine one. An evaluation of the enthalpy of the transformation measured by TDA leads to 0.044 eV/per formula unit. Because of the sizable errors in both techniques, the qualitative agreement can be considered as satisfactory. The fact that the transition is exothermic and irreversible is consistent with the fact that this phase is usually obtained at high temperature or in hydrothermal conditions.<sup>4</sup> VASP optimization of the olivine  $\text{NaFePO}_4$  structure converged readily toward the experimental parameters. This result demonstrates that this structure shows at least a strong enough relative stability not to be transformed into the maricite phase while cycling. Theoretical calculations also allowed us to determine the theoretical potential of a hypothetical plateau between  $\text{FePO}_4$  and  $\text{NaFePO}_4$  versus  $\text{Na}/\text{Na}^+$  (see the Supporting Information). The obtained value, 2.92 V, is in good accordance with equilibrium

(11) Nespolo, M.; Ferraris, G.; Ohashi, H. *Acta Crystallogr., Sect. B* **1999**, 55, 902–916.

(12) (a) Brown, I. D.; Shannon, R. D. *Acta Crystallogr., Sect. A* **1973**, 29, 266–282. (b) Robinson, K.; Gibbs, G. V.; Ribbe, P. H. *Science* **1971**,

172, 567–570.  $\Delta = \frac{1}{N} \sum_{i=1}^N [(d_i - \langle d \rangle) / \langle d \rangle]^2$  and  $\lambda = \frac{1}{N} \sum_{i=1}^N \left( \frac{d_i}{d_0} \right)^2$  characterize bond-length distortions with  $d_i$  the length of the bond  $i$ ,  $\langle d \rangle$  the average bond length,  $d_0$  the bond length of in a regular polyhedron and  $N$  the coordination number.  $\sigma = \frac{1}{m-1} \sum_{i=1}^m [(\theta_i - \theta_0)]^2$  characterizes the bond-angle distortion with  $(m, \theta_0)$  equal to (12, 90°) and (6, 109.47°) for octahedrons and tetrahedrons, respectively.

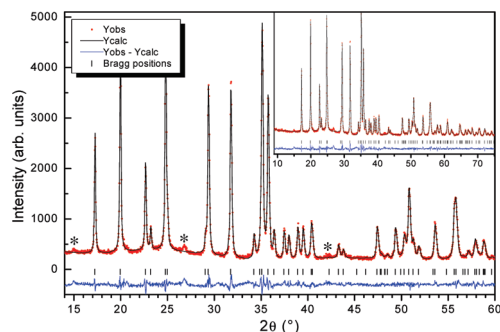


**Figure 5.** Rietveld refinement of  $\text{Na}_{0.7}\text{FePO}_4$  olivine structure obtained in oxidation at a 2.95 V potential. Asterisks denote possible superstructure peaks.

values (defined as the potential obtained upon relaxation to  $dV/dt < 0.1$  mV/h): 2.863 V on discharge and 2.869 V and 2.972 V on charge (Figure 2). We note that with respect to a  $\text{Li}/\text{Li}^+$  reference electrode (3.20 V), this value is substantially lower than that expected from the  $\text{Li}/\text{FePO}_4$  system (3.45 V). As mentioned above, a discontinuity in the potential-composition curve occurs in the vicinity of  $x = 0.65$  ( $\pm 0.05$ ) both on discharge (less visible) and on charge (Figure 2). This discontinuity corresponds to an electrochemical biphasic process involving a  $\text{Na}_{0.70}\text{FePO}_4$  phase in equilibrium with  $\text{FePO}_4$ , as confirmed by ex situ X-ray diffraction diagrams performed at  $x = 0.4$  (see the Supporting Information). Because the biphasic process is better defined on charge,  $\text{Na}_{0.7}\text{FePO}_4$  was obtained with high purity by equilibrating the sample at 2.95 V versus  $\text{Na}/\text{Na}^+$  (point B in Figure 2). The corresponding single phase ex situ X-ray diffraction diagram is presented in Figure 5. This diffraction pattern can be partially indexed with a *Pnma* orthorhombic unit-cell having parameters intermediate between those of  $\text{NaFePO}_4$  and  $\text{LiFePO}_4$ :  $a = 10.2886(7)$  Å,  $b = 6.0822(4)$  Å,  $c = 4.9372(4)$  Å, and  $V = 308.95(4)$  Å<sup>3</sup>. A consistent average structure is obtained from Rietveld refinement with, in particular, an occupancy for the sodium site (0.710(18)) in good agreement with the expected composition inferred from electrochemical experiments. However, the significant deviation of the calculated BVS from the theoretical values ( $\text{BVS}_{\text{Na}} = 0.736$ ,  $\text{BVS}_{\text{Fe}} = 2.083$ ,  $\text{BVS}_{\text{P}} = 5.181$ ) and the important anisotropic atomic displacement parameters for the sodium ( $U_{11} \approx 3U_{33}$  and  $U_{22} \approx 5U_{33}$ ) are the signature of a not fully resolved structure with probably the existence of a disorder. Extra diffraction peaks are in fact observed in the diffractogram (asterisks in Figure 5) and could correspond to a 5-fold superstructure in the  $c$  direction, although their limited intensity and number prevent a definitive answer from powder diffraction diagrams. Electron diffraction studies are in progress to confirm such a possibility.

Following thermal differential analysis,  $\text{Na}_{0.7}\text{FePO}_4$  is found to be stable up to 469 °C. It transforms into a

mixture of maricite  $\text{NaFePO}_4$  and alluaudite-type  $\text{NaFe}_{3.67}(\text{PO}_4)_3$  (composition close to  $\text{Na}_{0.3}\text{FePO}_4$ ),<sup>13</sup> as demonstrated by in situ X-ray diffraction experiments (see the Supporting Information). Alluaudite phases present one-dimensional sodium channels.<sup>14</sup> The similarities between the two structures suggest that, upon heating, some channels in the partially intercalated olivine are preserved, whereas others collapse to lead to the alluaudite phase. This transformation is still complex. In particular, pretransitional modifications can be observed around 430–470 °C, both in  $\text{NaFePO}_4$  (Figure 4) and  $\text{Na}_{0.7}\text{FePO}_4$  (see the Supporting Information). A full phase diagram determination is currently under way in order to determine the precise reaction path as well as to allow a comprehensive comparison with the  $\text{FePO}_4/\text{LiFePO}_4$  system.<sup>15</sup>

The occurrence of an intermediate phase while cycling in the case of sodium, whereas intermediate compositions for lithium iron phosphate were only characterized in special conditions,<sup>16</sup> illustrates the increased interaction of sodium ions compared to lithium ions with the host structure. A similar behavior is observed by comparing the number of phases obtained in  $\text{Li}_x\text{CoO}_2$ <sup>17</sup> compared to  $\text{Na}_x\text{CoO}_2$ .<sup>18</sup>

Two new  $\text{Na}_x\text{FePO}_4$  phases ( $x = 0.7$ ,  $x = 1$ ) were electrochemically synthesized and their olivine-based structures reported. Electrochemical tests of carbon coated  $\text{FePO}_4$  powders in sodium batteries are currently in progress. Good cycling properties, as well as noticeable differences with the lithium equivalent  $\text{LiFePO}_4$ , will hopefully motivate further studies in order to develop sodium battery technologies based on olivine iron phosphates. Future work will also focus on finding out whether these new phases present interesting physical properties.

**Acknowledgment.** The authors thank M. Cuisinier (IMN, Nantes, France) for providing the initial  $\text{LiFePO}_4$  powders.

**Supporting Information Available:** X-ray Rietveld refinements data for  $\text{NaFePO}_4$  and  $\text{Na}_{0.7}\text{FePO}_4$  with crystallographic information files (CIF) for both phases; cell parameter evolution for temperature-dependent experiment performed on  $\text{NaFePO}_4$ ; DFT program details for calculated stability of phases and results of the geometry optimization, structural characterization of the  $\text{Na}_{0.4}\text{FePO}_4$  composition, temperature-dependent in situ X-ray diffraction diagrams, and thermal differential analysis obtained for  $\text{Na}_{0.7}\text{FePO}_4$  (PDF). This material is available free of charge via the Internet at <http://pubs.acs.org>.

(13) Korzenski, M. B.; Schimek, G. L.; Kolis, J. W.; Long, G. J. *J. Solid State Chem.* **1998**, *139*, 152–160.

(14) Leroux, F.; Mar, A.; Payen, C.; Guyomard, D.; Verbaere, A.; Piffard, Y. *J. Solid State Chem.* **1995**, *115*, 240–246.

(15) Delacourt, C.; Poizot, P.; Tarascon, J.-M.; Masquelier, C. *Nat. Mater.* **2005**, *4*, 254–260.

(16) Delacourt, C.; Rodríguez-Carvajal, J.; Schmitt, B.; Tarascon, J.-M.; Masquelier, C. *Solid State Sci.* **2005**, *7*, 1506–1516.

(17) Reimers, J. N.; Dahn, J. R. *J. Electrochem. Soc.* **1992**, *139*, 2091–2097.

(18) Molenda, J.; Delmas, C.; Dordor, P.; Stoklosa, A. *Solid State Ionics* **1984**, *12*, 473–477.